Received: 20 February 2023 | Revised: 2 February 2024 | Accepted: 5 March 2024

DOI: 10.1111/exd.15084

Experimental Dermatology WILEY

RESEARCH ARTICLE

CLDN1 knock out keratinocytes as a model to investigate multiple skin disorders

Kimberly A. Arnold[1] | Mary C. Moran[1,2] | Huishan Shi[1] | Ivonne M. J. J. van Vlijmen-Willems[3] | Diana Rodijk-Olthuis[3] | Jos P. H. Smits[3,4] | Matthew G. Brewer[1]

[1]Department of Dermatology, University of Rochester Medical Center, Rochester, New York, USA

[2]Department of Microbiology and Immunology, University of Rochester Medical Center, Rochester, New York, USA

[3]Department of Dermatology, Radboud University Medical Center, Radboud Institute for Molecular Life Sciences (RIMLS), Nijmegen, The Netherlands

[4]Department of Dermatology, University Hospital Düsseldorf, Medical Faculty, Heinrich Heine University, Düsseldorf, Germany

Correspondence
Matthew G. Brewer, Department of Dermatology, University of Rochester Medical Center, 601 Elmwood Ave Box 697, Rochester, NY, 14642 USA.
Email: matthew_brewer@urmc.rochester.edu

Abstract

The transmembrane protein claudin-1 is critical for formation of the epidermal barrier structure called tight junctions (TJ) and has been shown to be important in multiple disease states. These include neonatal ichthyosis and sclerosing cholangitis syndrome, atopic dermatitis and various viral infections. To develop a model to investigate the role of claudin-1 in different disease settings, we used CRISPR/Cas9 to generate human immortalized keratinocyte (KC) lines lacking claudin-1 (CLDN1 KO). We then determined whether loss of claudin-1 expression affects epidermal barrier formation/function and KC differentiation/stratification. The absence of claudin-1 resulted in significantly reduced barrier function in both monolayer and organotypic cultures. CLDN1 KO cells demonstrated decreases in gene transcripts encoding the barrier protein filaggrin and the differentiation marker cytokeratin-10. Marked morphological differences were also observed in CLDN1 KO organotypic cultures including diminished stratification and reduced formation of the *stratum granulosum*. We also detected increased proliferative KC in the basale layer of CLDN1 KO organotypic cultures. These results further support the role of claudin-1 in epidermal barrier and suggest an additional role of this protein in appropriate stratification of the epidermis.

KEYWORDS
atopic dermatitis, claudin-1, keratinocytes, tight junctions

1 | INTRODUCTION

The skin serves as an integral barrier between an organism and harmful external stimuli such as allergens, chemicals and infectious agents. Keratinocytes (KC), the primary cell of the epidermis, differentiate to form the stratified squamous epithelia responsible for the structure and barrier function of the skin. The layers of the epidermis (from the most internal to superficial) include: the *stratum basale*, *stratum spinosum*, *stratum granulosum* (SG) and *stratum corneum* (SC). These layers form two major lines of defence for the body; the outermost 'brick and mortar' structure of anucleate KC (corneocytes) and intercellular lipids within the SC and tight junctions (TJ) within the SG.[1,2] In addition to forming epidermal barrier, KC are highly responsive to skin perturbations through production of cytokines and chemokines.[3,4] Both barrier function and production of immune modulating molecules are key characteristics of KC that protect the skin from pathogens.

Claudin-1 is an important TJ protein expressed by KC that has been strongly implicated in barrier function and disease states. In global claudin-1 knock-out mice, offspring have severely compromised epidermal barrier, as demonstrated by elevated transepidermal

Abbreviations: CLDN, claudin; EIS, electrical impedance spectroscopy; FD, fluorescein isothiocyanate-dextran; KC, keratinocytes; KO, knock out; SC, stratum corneum; SG, stratum granulosum; sgRNA, single-guide RNA; TEER, transepithelial electrical resistance; TJ, tight junction.

Jos P. H. Smits and Matthew G. Brewer contributed equally to this study.

water loss and death shortly after birth.[5] Additional studies in animals and cells using partial knock out/knock down techniques demonstrated that the expression level of claudin-1 directly related to the magnitude of barrier function developed by KC.[6,7] Animals with the most diminished claudin-1 expression demonstrated altered skin characteristics, including thickening of the epidermal compartment, elevated influx of immune cells and increased expression of inflammatory cytokines and chemokines.[7] The impact of diminished claudin-1 expression on epidermal barrier function has also been demonstrated in humans. A mutation in *CLDN1* is responsible for neonatal ichthyosis and sclerosing cholangitis, which is characterized by substantial epidermal paracellular permeability.[8] Furthermore, decreased claudin-1 expression is associated with atopic dermatitis (AD), a common skin disorder characterized by epidermal barrier dysfunction.[6,9] Additional important characteristics of these diseases include altered epidermal morphology and changes to the inflammatory signature of the epidermis. Taken together, these observations support that robust epidermal barrier, and specifically the presence of claudin-1, is fundamental for healthy skin function. Whether altered claudin-1 expression impacts other epidermal characteristics such as cytokine production or correct epidermal stratification is poorly defined.

Given the importance of claudin-1 in barrier function and its contribution to multiple human diseases, we determined whether loss of claudin-1 expression altered different aspects of KC biology in monolayer (barrier function and gene expression) and organotypic cultures (barrier function, morphological changes, protein expression and proliferation). To investigate this, we generated claudin-1 knockout (CLDN1 KO) cells in the immortalized human KC line N/TERT-2G[10] using CRISPR/Cas9. We hypothesized that claudin-1 loss would abrogate barrier function due to poorly formed TJs and impair the formation of fully stratified epidermis. A better understanding of the relationship between claudin-1 expression and epidermal structure/function is critical in identifying mechanisms that contribute to disease pathology.

2 | RESULTS

To investigate the importance of claudin-1 expression in human skin barrier formation and keratinocyte differentiation/stratification, we created cell lines lacking claudin-1 via electroporation-mediated delivery of CRISPR/Cas9 gene-editing components. To accomplish this, the immortalized human KC cell line N/TERT-2G was used because we have shown that it faithfully recapitulates primary KC characteristics of differentiation, barrier formation and TJ organization.[11,12] A CRISPR/Cas9 system containing three single-guide RNAs (sgRNA) targeting the first exon of *CLDN1* and recombinant Cas9 nuclease was used to knockout claudin-1 expression (Figure 1A). A ribonucleoprotein complex of Cas9 protein and sgRNAs was chosen because there is low off-target editing due to the short half-life of Cas9 protein in cells,[13] in contrast to other delivery methods such as plasmids or viral vectors,[14] which have prolonged expression of the gene editing complex. Additionally, multiple sgRNAs were chosen to ensure high knockout efficiency from a single editing event. While CRISPR/Cas9 editing with a single sgRNA can result in re-ligation of the Cas9-induced dsDNA break, multiple sgRNAs facilitate large deletions in the target gene, improving editing efficiency.[15,16] This was observed by an apparent complete KO of *CLDN1* (i.e. the absence of a WT band by PCR) after a single instance of CRISPR/Cas9-mediated gene editing (Figure 1). Cells exposed to the CRISPR/Cas9 components were analysed by PCR and gel electrophoresis to determine the sequence modification to *CLDN1*. Three sizes of predicted deletions (37, 83 and 140 bp) were expected to occur in CRISPR/Cas9 edited cells based on the regions targeted by the sgRNAs. The polyclonal population of edited cells demonstrated a triple banding pattern after PCR amplification of the targeted *CLDN1* loci (Figure 1B). Two of these bands corresponded to the expected deletions (~484 bp; 83 nucleotide deletion, ~427; 140 nucleotide deletion) while the smallest deletion (~530 bp) was not detected (Figure 1A). The third unanticipated band suggests an alternative protospacer adjacent motif site was utilized for gene editing, resulting in a slightly smaller gene product than the 484 bp band. No changes in band size were observed in WT cells exposed to the Cas9 protein alone. Claudin-1 expression in WT and CLDN1 KO cells was then assessed by western blot analysis. *CLDN1* edited polyclonal N/TERT-2G cells (pCLDN1 KO) had an undetectable level of claudin-1 expression after differentiation, indicating a high degree of editing efficiency in agreement with PCR results (Figure 1B,C). As polyclonal populations of cells may demonstrate variability in downstream assays due to a mixture of edited and unedited cells (i.e. some cells still expressing claudin-1), clonal selection from the pCLDN1 KO population was performed to isolate individual clones. We successfully isolated multiple CLDN1 KO clones which we called 'A8', 'H1' and 'D5' and then validated via PCR, DNA sequencing and western blot (Figure S1). Sanger sequencing indicated that the A8 clone had a 120 bp deletion while both H1 and D5 had a 42 and 43 bp deletion, respectively (Figure S1B). Additionally, western blot analysis demonstrated no detectable claudin-1 expression in either the A8, H1 or D5 clone cells (Figure S1C).

We first investigated whether deletion of *CLDN1* affected formation of KC barrier as claudin-1 expression has been strongly implicated in barrier function of human and mouse skin.[5,9] Monolayer cell cultures lacking claudin-1 expression (pCLDN1 KO) demonstrated impaired barrier formation as measured by decreased transepithelial electrical resistance (TEER) at multiple days post differentiation (Figure 2A). We then confirmed these changes in CLDN1 KO clonal lines to ensure that our observations persisted in cells with a single genetic background. Each of the CLDN1 KO clones demonstrated reduced TEER development compared to a WT clone, in accordance with our polyclonal findings (Figure 2A). To determine whether the change in TEER was reflected in movement of larger molecules through the monolayer, permeability assays using either small (4 kDa–FD4) or large (40 kDa–FD40) FITC-dextran macromolecules were used.[17] As KC lacking claudin-1 differentiated, the permeability assay with FD4 showed a reproducible decrease in barrier function, with FD4 flux being higher in pCLDN1 KO cells at both 2 and

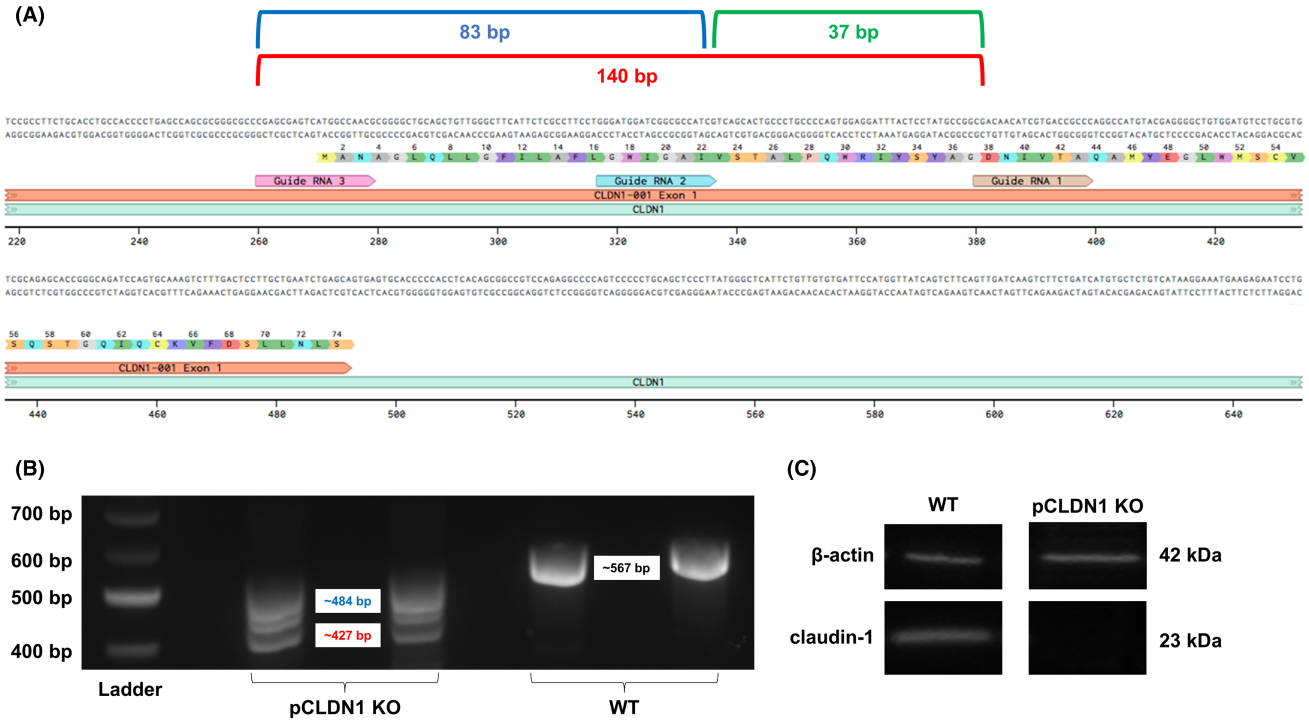

FIGURE 1 CRISPR/Cas9-based knock out of *CLDN1* in immortalized keratinocytes. (A) Schematic of single-guide RNA (sgRNA) locations in *CLDN1* sequence used to knock out claudin-1 expression in the immortalized keratinocyte (KC) line N/TERT-2G. (B) PCR amplification and gel electrophoresis of edited *CLDN1* compared to wildtype (WT), expected at 567 base pairs (bp). Two of the three combinations of sgRNA-targeted cuts are indicated at ~427 and ~484 bp. (C) Western blot expression of claudin-1 in the polyclonal knock out (pCLDN1 KO) versus WT.

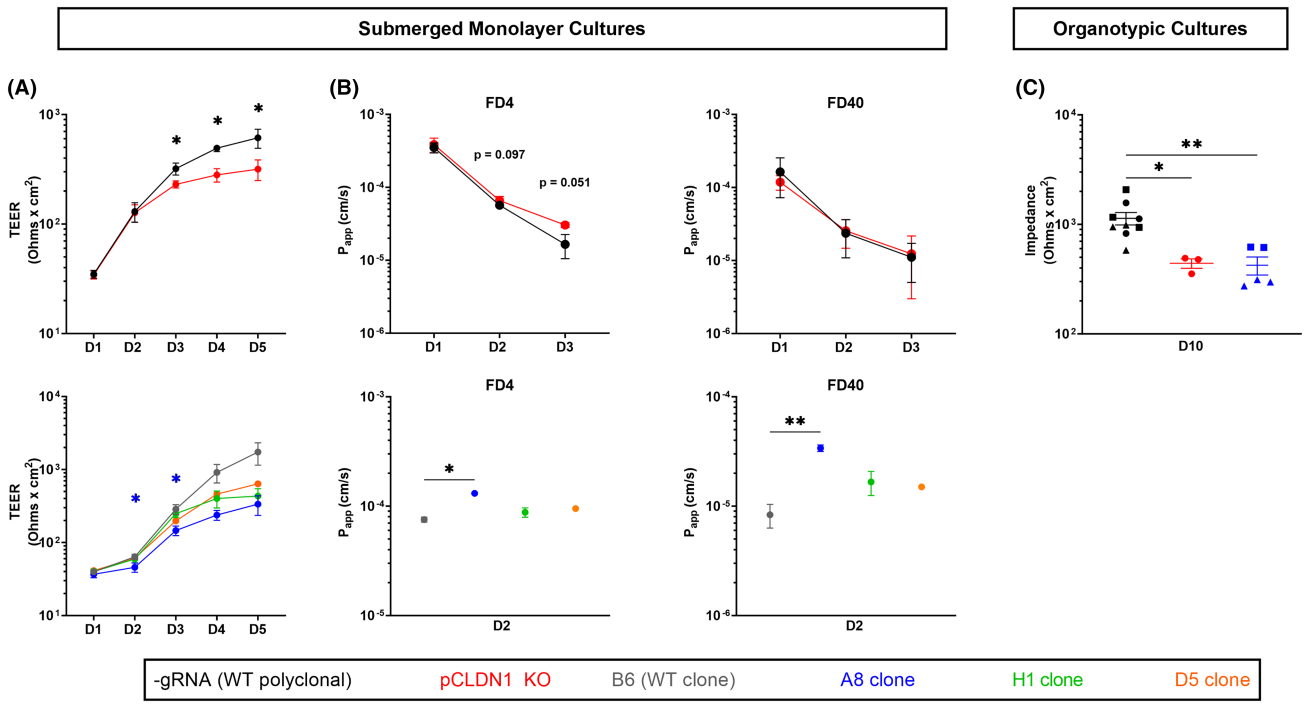

FIGURE 2 Knock out of *CLDN1* diminishes barrier integrity in submerged N/TERT-2G monolayer and organotypic cultures. Submerged monolayer cell cultures were differentiated in high Ca^{2+} containing media. Barrier function was quantified by (A) transepithelial electrical resistance (TEER) every day post differentiation for 5 days or (B) permeability assays at 1, 2 and 3 days post differentiation. WT, pCLDN1 KO and A8 clone cells were used to develop organotypic cultures and (C) electrical impedance was measured 10 days after being lifted to the air–liquid interface. -gRNA, pCLDN1 KO $n=4$ experiments in (A, B). B6, A8, H1 clones $n=3$ experiments and D5 clone $n=1$ experiment in (A, B). $n=3$–9 total constructs from three experiments with different symbols representing individual experiments (C). Statistical differences were evaluated against the relevant WT control by either a paired *t*-test (A, B) or an ANOVA (A, B, C). Data are shown as mean ± SEM. $^{*}p<0.05$, $^{**}p<0.01$.

3 days post differentiation (Figure 2B). No change in FD40 flux was detected between the WT and pCLDN1 KO cells (Figure 2B). A similar difference in FD4 flux across the monolayer was detected with clonal cells at Day 2 (Figure 2B). Of note, we did detect a significant difference in FD40 flux between WT and CLDN1 KO clone cells in contrast to our findings with polyclonal cells (Figure 2B), suggesting that low levels of claudin-1 expression in polyclonal cells may limit larger macromolecule flux across the cell monolayer. To extend our observations, air–liquid interface organotypic cultures were made from WT, pCLDN1 KO or A8 clone cells to model the stratified structure of the epidermis.[12] Organotypic cultures were allowed to stratify for 10 days and then electrical impedance spectroscopy (EIS) was used to assess barrier function. In both pCLDN1 KO and A8 clone organotypic cultures, a significant decrease in electrical impedance (a measurement of barrier integrity, comparable to TEER) was observed, recapitulating the findings from submerged monolayer cultures (Figure 2C).

Diminished claudin-1 expression is observed in complex disease states (such as AD) where other defects in KC biology such as differentially expressed genes, microbial dysbiosis and epidermal barrier dysfunction are detected.[18–20] To test whether claudin-1 expression mediates some of these changes, qPCR was used to assess transcript levels of genes encoding barrier proteins, differentiation markers or cytokines in monolayer cultures undergoing differentiation. Transcript levels of representative barrier proteins (claudin-4, claudin-23,[21,22] filaggrin and occludin), differentiation markers (cytokeratin-10, transglutaminase-1, cytokeratin-5, involucrin and loricrin) and cytokines (IL-1β, IFNα1, IL-8, IL-25, IL-33 and TSLP) reported in the literature to be important for epidermal function and responsiveness were compared between WT and pCLDN1 KO cells. Contrary to our hypothesis, most of these transcripts (*CLDN23*, *OCLN*, *KRT5*, *IVL*, *LOR*, *CXCL8*, *IL25*, *IL33* and *TSLP*) remained unchanged (not shown) in pCLDN1 KO cells compared to WT levels. However, decreased expression was detected in *KRT10* and *FLG* at Day 2 of KC differentiation in pCLDN1 KO cells (Figure 3). We did observe pronounced changes in expression over the course of differentiation for many of the genes investigated, indicating that after exposure to high Ca^{2+} concentrations, KC underwent extensive changes in transcriptional activity (Figure S2). This is shown by a change in expression of the genes (*CLDN4*, *KRT10*, *TGM1* and *FLG*) from positive (low expression) ΔCq values to close to zero/negative (high expression) ΔCq values (Figure S2). We also confirmed that gene expression during differentiation was similar between pCLDN1 KO cells and the three clones we isolated (Figure S3), supporting that the observed differences were maintained in cell lines containing a single mutation in *CLDN1*. Collectively, these observations indicate that claudin-1 expression may increase expression of select genes important for various functions of KC including differentiation and barrier function.

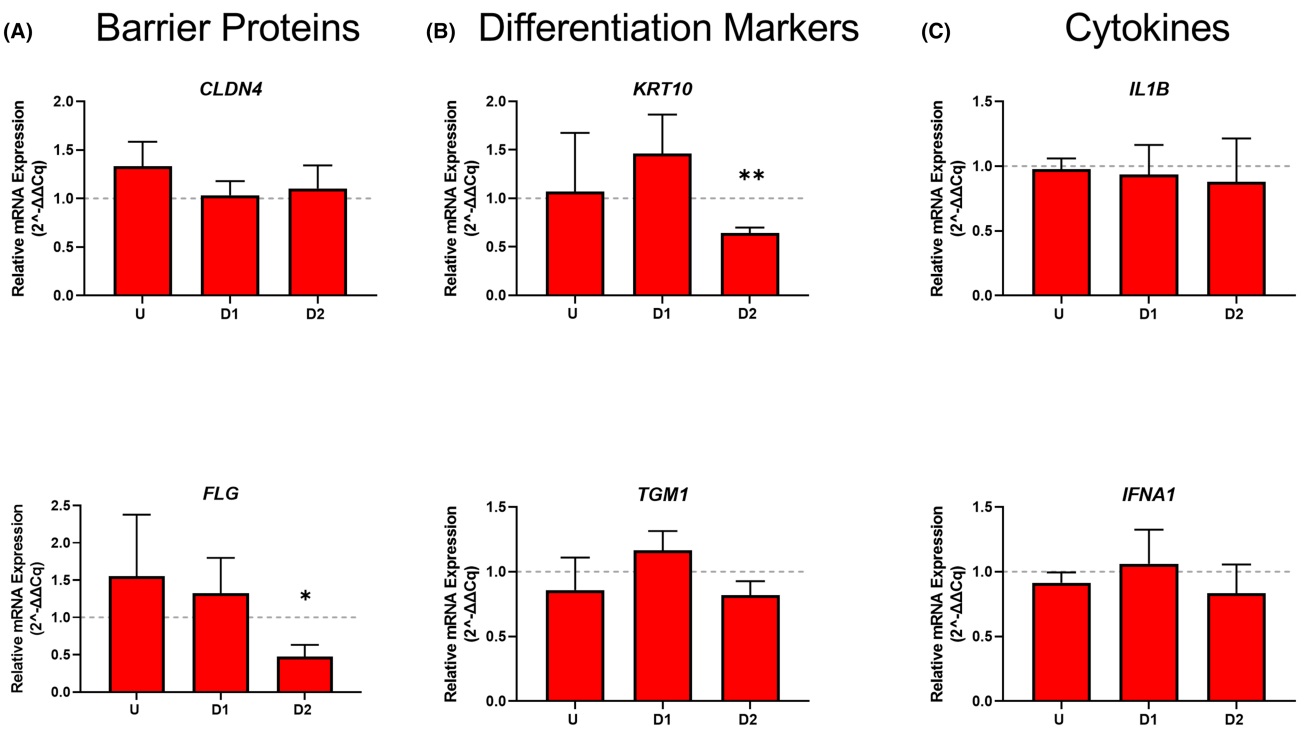

FIGURE 3 *CLDN1* knock out diminishes mRNA expression of genes involved in KC differentiation and barrier function. Relative gene expression of representative (A) barrier proteins, (B) differentiation markers and (C) cytokines in undifferentiated and early differentiated submerged monolayer cultures of KC. Gene expression levels measured by qPCR are represented as $2^{-\Delta\Delta Cq}$ compared to WT ($n = 5$ experiments). Gene of interest expression was normalized to expression of the housekeeping gene *HPRT1*. The dashed grey line represents normalized WT transcript levels. Statistical differences were evaluated by a paired *t*-test. Data are shown as mean ± SEM. $^{*}p < 0.05$, $^{**}p < 0.01$.

To determine whether claudin-1 expression impacted appropriate stratification during differentiation, air-liquid interface organotypic cultures were used.[12] Organotypic cultures were stained with haematoxylin and eosin (H&E) to observe morphological differences. Cultures derived from pCLDN1 KO cells and A8 clone cells demonstrated parakeratosis (nuclei in the stratum corneum), reduced stratification and a diminished granular layer by both size and the appearance of granule containing cells (Figure 4A). We then quantified the total thickness of the organotypic cultures and the thickness of the stratum corneum layer. WT organotypic cultures had greater total thickness, but a trend in reduced *stratum corneum* thickness when compared to cultures derived from claudin-1 lacking cells (either pCLDN1 or A8, Figure 4B). When the ratio of these two metrics was compared, it was supportive of *stratum corneum* thickening in constructs derived from claudin-1 lacking cells, as values were consistent across polyclonal and monoclonal cells and ~2-fold greater than wildtype controls (Figure 4B). We also stained organotypic cultures from A8 clone cells for Ki67, claudin-1, claudin-4, filaggrin and involucrin. In confirmation of our successful isolation of a claudin-1 lacking clone, no claudin-1 expression was observed in the organotypic cultures derived from the A8 clone (Figure 5A). Staining for claudin-4 and filaggrin, known contributors to skin structure and barrier, showed reduced expression in the A8 clone organotypic cultures compared to WT (Figure 5B). These observations suggest that the reduction in TEER, EIS, and/or permeability (Figure 2) could result from decreased expression of multiple barrier proteins.

Diminished stratification (Figure 4A,B) and parakeratosis could be attributed to altered KC proliferation. For that reason, Ki67, a known marker of proliferation,[23] staining was utilized to assess proliferative capacity of organotypic cultures from both WT and CLDN1 KO cells (Figure 5A). 2 of the 3 organotypic cultures derived from A8 cells demonstrated increased Ki67^{+} staining in the basal layer compared to WT (Figure 5B). Taken together, these results suggest that expression of claudin-1 contributes to additional aspects of keratinocyte biology including differentiation and stratification.

3 | DISCUSSION

In agreement with previous literature,[5,6,9,24,25] these studies further confirm claudin-1 as a key contributor to barrier function of the skin. Importantly, our results demonstrate that KC completely lacking claudin-1 still develop barrier function as they differentiate, which was observed by an increase in TEER over the course of differentiation (Figure 2). This indicates that other claudins or barrier proteins are able to establish functional barrier in KC even in the absence of claudin-1. There are other claudins that have been detected in KC, or diminished in AD, such as claudin-4, claudin-12, claudin-23 and/or claudin-25, which could provide the residual barrier function observed in our models.[9,26]

Loss of claudin-1 diminished expression of the transcripts for *KRT10* and *FLG* (Figure 3). Another study using siRNA knockdown of claudin-1 demonstrated a transient increase in *IL1B* expression

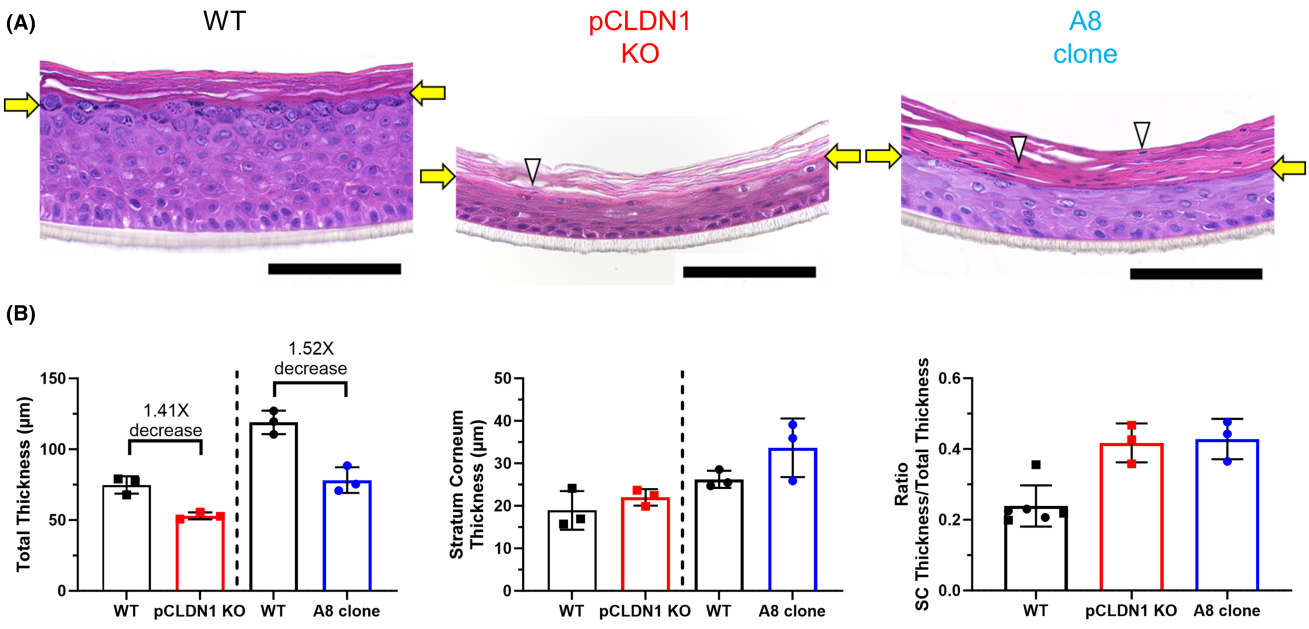

FIGURE 4 Organotypic cultures lacking claudin-1 demonstrate impaired stratification. WT, pCLDN1 KO and A8 clone cells were used to create organotypic cultures. 10 days after being lifted to the air–liquid interface they were (A) visualized with haematoxylin and eosin staining and (B) quantified for total and stratum corneum thickness using ImageJ. The ratio of these values was also calculated. The white arrow heads denote sites of parakeratosis (nuclei in the stratum corneum) while the yellow arrows indicate the stratum granulosum or lack thereof in the pCLDN1 KO and A8 clone cultures. Scale bar = 100 µm. Images from representative organotypic cultures from experiments with either pCLDN1 KO cells or A8 clone cells. Data are shown as individual cultures with mean ± SD.

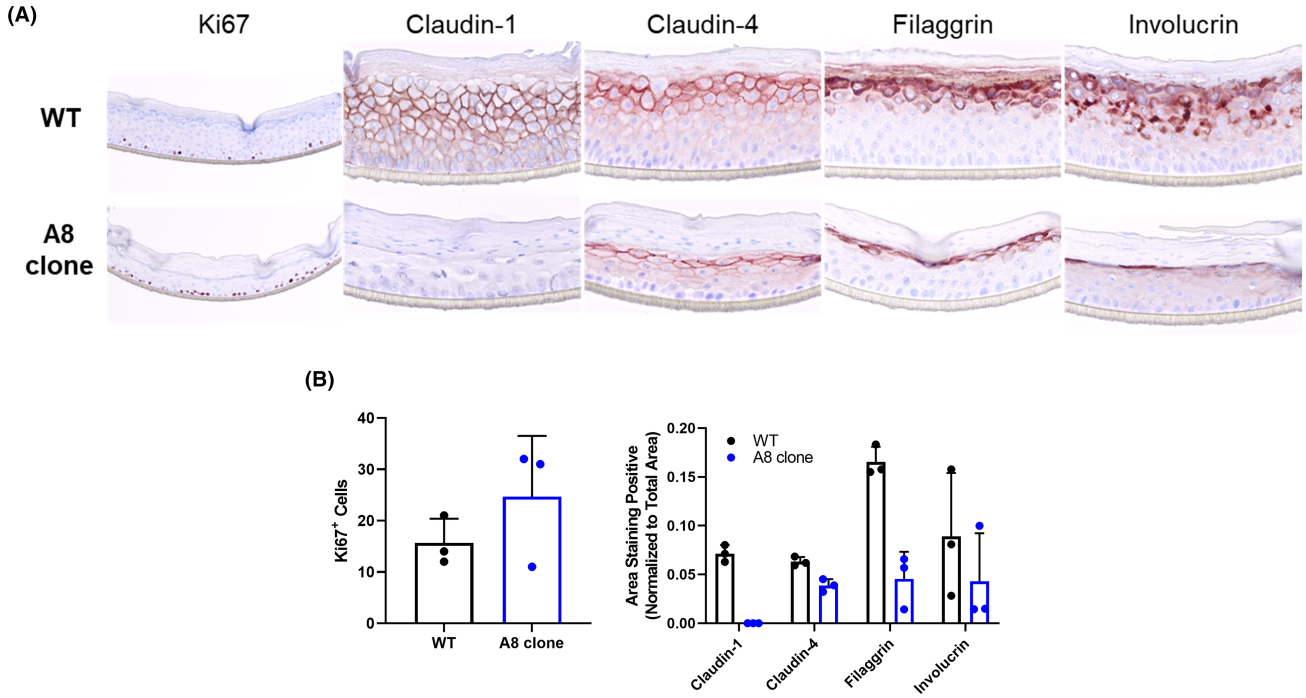

FIGURE 5 Claudin-1 lacking KC have altered expression of differentiation associated proteins in organotypic cultures. WT and CLDN1 KO A8 clone cells were used to create organotypic cultures. Ten days after being lifted to the air–liquid interface they were (A) stained for Ki67, claudin-1, claudin-4, filaggrin or involucrin and then (B) quantified for the cells or area positively staining for the different proteins with ImageJ and then normalized to total area. Images from one representative organotypic culture from $n = 3$. Data are shown as individual cultures (symbols) with mean ± SD.

(~3.5-fold) acutely after differentiation,[6] conflicting with our observation that *IL1B* was unaffected. Two important differences between this study and ours exist, including the method used to alter claudin-1 expression (CRISPR/Cas9 versus siRNA) and the cell culture model (monolayer versus organotypic cultures). Of note, Bergmann et al mentioned that they detected a transient decrease in *CLDN4* expression (<2-fold), while expression of *TJP1* (gene encoding ZO-1), *F11R* (gene encoding JAM-A) and *OCLN* was unchanged, which was consistent with our observations of modest/few gene changes in CLDN1 KO cells. It was surprising that gene expression changes in KC lacking claudin-1 were limited since the CLDN1 KO mouse and humans with neonatal ichthyosis and sclerosing cholangitis demonstrate profound changes to the epidermal compartment, such as barrier dysfunction and altered *stratum corneum* morphology. Though some transcript changes reached statistical significance, those that did were less than a twofold change. As monolayer cultures have limited stratification and shorter time scales of differentiation (≤5 days vs. 10 days for organotypic culture studies) the absence of claudin-1 may not impact them as robustly as stratified models. This agrees with the pronounced changes seen in claudin-4 and filaggrin protein expression between the organotypic cultures lacking claudin-1 and WT controls, compared to the more modest changes detected in monolayer experiments.

Cells lacking expression of claudin-1 demonstrated reduced stratification and a poorly formed *stratum granulosum*, the layer where TJ occur,[27] which could contribute to why decreased TEER/EIS was detected in the two model systems investigated. Decreased claudin-1 expression in individuals with cutaneous disease such as neonatal ichthyosis and sclerosing cholangitis and AD[8,9] has been thought to promote elevated epidermal permeability due to diminished TJ function. Our observations suggest there could also be the added complication of altered differentiation and/or stratification of the epidermal compartment (Figure 4). Importantly, individuals with skin diseases demonstrating barrier impairment (such as AD), and mice with altered claudin-1 expression, have a thickened epidermal compartment,[7,28] which contrasts with our observations from claudin-1 lacking organotypic cultures. We attribute this difference to inflammation resulting from external stimuli able to penetrate the leaky epidermal barrier and activate the underlying host cells. Inflammation is thought to contribute to epidermal thickening, which is most notable in psoriatic skin, but also observed in other chronic inflammatory diseases such as AD.[29–31] Therefore, we hypothesize that topical application of a stimuli (such as a bacterium or cytokine) to organotypic cultures lacking claudin-1 would elicit an inflammatory response from KC and lead to greater stratification or thickening of organotypic cultures. This model of CLDN1 KO cells may prove useful for investigators trying to better understand the consequences of epidermal barrier disruption on human diseases that have altered epidermal morphology.

Organotypic cultures derived from cells lacking claudin-1 also demonstrated parakeratosis, a condition correlated with improper KC differentiation and observed in multiple chronic inflammatory

skin diseases including psoriasis and AD.[32,33] This observation is in accordance with qPCR analysis of differentiation dependent genes, which showed alterations at early stages of differentiation in cells lacking claudin-1 (Figure 3). To date, a link between claudin-1 expression and KC differentiation has been incompletely studied. Our results with organotypic cultures lacking claudin-1 suggest that claudin-1 may play a role in this process, which we observed through altered protein expression of differentiation markers (filaggrin, claudin-4) and increased $Ki67^{+}$ cells in the basal layer of CLDN1 KO constructs (Figure 5). These results indicate that expression of claudin-1 in KC may influence barrier function not only through its function in tight junctions, but also through promoting appropriate KC differentiation.

By obtaining a better understanding of the role epidermal barrier proteins play in KC differentiation and cutaneous barrier function, we can advance toward personalized therapeutics for individuals with acute and/or chronic skin conditions in which these barrier proteins are decreased. Restoring or increasing claudin-1 levels may be an important factor in barrier impaired diseases, such as AD, which could provide a new focus for novel therapeutics. Many therapies that improve AD, such topical and systemic steroids, monoclonal antibodies (dupilumab and tralokinumab) and Janus kinase inhibitors (ruxolitinib, abrocitinib and upadacitinib) primarily work through altering the host immune compartment.[34–36] While some of these interventions do increase expression of barrier molecules, this is most likely a by-product of dampening inflammation in the skin and not direct interaction with KC.[37] An example of directly influencing KC differentiation to improve barrier would be targeting the aryl hydrocarbon receptor by coal tar therapy or Tapinarof.[38–40] Concomitant therapies that actively promote barrier formation in the skin and dampen inflammation may be necessary in achieving the most beneficial disease outcomes. Going forward, as more information on the importance of claudin-1 and other claudin proteins in the epidermal environment is acquired, a better sense of the molecular changes necessary to promote robust barrier function and diminish disease associated pathology will be achieved.

4 | MATERIALS AND METHODS

4.1 | Cells

N/TERT-2G cells were propagated as previously described[10,12] at 37°C with 5% CO_2. N/TERT-2Gs were propagated in keratinocyte serum-free media (KSFM) 1X (Invitrogen/Gibco, Grand Island, NY, USA) with penicillin/streptomycin and amphotericin B (Invitrogen/Gibco). Cells were grown to 30% confluency and then trypsinized and plated in a 24-well plate at 1.5×10^5 cells per well for the following assays. Undifferentiated cells were left in KSFM and differentiated cells were switched to high-calcium [1.8 mM] (Boston Bioproducts, Ashland, MA) DMEM media (Thermo Fisher Scientific, Waltham, MA, USA) to induce differentiation.[41] Every 2 days, cells received fresh media.

4.2 | CRISPR/Cas9 editing of keratinocytes

A CRISPR/Cas9 knockout kit targeting *CLDN1* (Gene Knockout Kit v2) was obtained through Synthego (Synthego, Redwood City, CA, USA). The kit consisted of recombinant Cas9 protein and three sgRNAs with the following sequences: (1) CGACAACAUCGUGACCGCCC, (2) CGAUGGCGCCGAUCCAUCCC and (3) CGAGCGAGUCAUGGCCAACG. sgRNAs and Cas9 protein mixtures (ribonucleoprotein complex) were prepared per Synthego's instructions. For electroporation, the Neon Transfection System (ThermoFisher Scientific) was filled with 3 mL of electrolytic buffer and the following settings were used: voltage = 1400 V, width = 20 ms, pulses = 2. Cells were trypsinized with TrypLE (ThermoFisher Scientific), neutralized with DMEM containing 10% fetal bovine serum, and centrifuged at 1250 RPM for 5 min. 5×10^5 cells were pelleted, and the supernatant was removed. Cells were then resuspended in 12 μL of 3:1 resuspension buffer R and pre-mixed RNP. Ten microlitres of the reaction mix was used for electroporation. Electroporated cells were added to 6-well plate containing prewarmed media and expanded.

4.3 | DNA Isolation, PCR and gel electrophoresis

Cells from CRISPR/Cas9 editing reaction were expanded from a 6-well plate to a 25 cm^2 tissue culture flask at which point 10^6 cells were processed for genomic DNA isolation using the PureLink Genomic DNA Mini Kit (ThermoFisher Scientific). Isolated DNA was resuspended in nuclease free water and quantified by UV–Vis absorbance using a SpectraDrop Micro-Volume Microplate (Molecular Devices, San Jose, CA, USA). Next, PCR was used to amplify the edited region of *CLDN1*. Each PCR reaction contained 7 μL of nuclease free water, 10 μL of Accustart (Quantabio, Beverly, MA, USA), 2 μL of primer mix (Forward: AACCCCGACCCAGAGCTTCTCC, Reverse: GGGCGTCGCTTTCCTCAAACCA) at 10 μM and 1 μL of gDNA at 10 ng/μL. PCR amplification for *CLDN1* was done using a SimpliAmp Thermal Cycler (ThermoFisher Scientific) with the following protocol: 95°C for 10 min, 30 cycles (95°C for 30 s, 58°C for 30 s, 72°C for 1 min), 72°C for 7 min, end at 4°C. After PCR was performed, 8 μL of product was added to a 2.5% agarose gel containing GelRed Nucleic Acid Gel Stain (Biotium, Fremont, CA, USA) and ran for 2 h at 80 V. Gels were imaged using a BioRad Gel Imaging System (Bio-Rad, Hercules, CA, USA) and the bands of interest were excised. DNA was extracted from the agar using a QIAquick Gel Extraction Kit (Qiagen, Hilden, Germany). Isolated DNA was sequenced (Genewiz, Plainfield, NJ, USA) using the same primers from the amplification step.

4.4 | Monoclonal selection of CLDN1 KO cells

pCLDN1 KO cells were trypsinized, centrifuged and then resuspended in KSFM media. Five-hundred cells were added to the uppermost left well of a 96-well plate. Twofold dilutions were performed

down the first column of the plate followed by twofold dilutions across all rows of the plate. Wells that contained a single cell were used for clonal selection, grown to ~30% confluency and expanded. Clonality was confirmed by PCR and Sanger sequencing as above.

4.5 | Organotypic culture model

Organotypic cultures were generated using 24-well cell culture inserts (Nunc, ThermoFisher Scientific) coated with rat tail collagen (100 μg/mL, BD Biosciences, Franklin Lakes, NJ, USA) at 4°C for 1 h prior to seeding of 150 000 N/TERT-2G WT, pCLDN1 KO, or CLDN1 KO clone A8 KC in 150 μL CnT-prime medium (CELLnTEC, Bern, Switzerland). After 48 h, cell culture medium was switched to 3D differentiation medium for another 24 h, consisting of 60% CnT-Prime 3D Barrier medium (CELLnTEC) and 40% high-glucose Dulbecco's modified Eagle's medium (DMEM, Sigma-Aldrich, St. Louis, MO, USA). Thereafter, the organotypic cultures were lifted to the air-liquid interface, with differentiation medium refreshed every other day. At Day 10, impedance values were measured and then organotypic cultures were fixed in 4% formalin solution for 4 h and subsequently embedded in paraffin. Six micrometer sections were stained with haematoxylin and eosin (H&E, Sigma-Aldrich). Antibodies against claudin-1 (rabbit anti-claudin-1, ThermoFisher Scientific, #51-9000, 1:200 diluted), claudin-4 (mouse anti-claudin-4, ThermoFisher Scientific, #32-9400, 1:200 diluted), filaggrin (mouse anti-filaggrin, ThermoFisher Scientific, #MA5-13440, 1:100 diluted), involucrin (mouse anti-involucrin, produced in house at Radboud University, 1:20 diluted) and Ki67 (rabbit anti-Ki67, Abcam, Cambridge, UK, ab16667, 1:200 diluted) were used in combination with goat anti-rabbit (Vector laboratories, Burlingame, CA, USA) and horse anti-mouse (Vector laboratories) antibodies as described before.[12] Quantification of organotypic culture thickness and *stratum corneum* thickness was performed as previously described.[42] Images taken at 20X magnification were analysed using ImageJ (software version 2.1.0) to count $Ki67^+$ cells. To quantify epithelial staining, we adapted the methodology from https://imagej.nih.gov/ij/docs/examples/stained-sections/index.html. Organotypic cultures stained for expression of claudin-1, claudin-4, filaggrin or involucrin and then captured at 40X and imported into ImageJ. For each image, the functions to run an RGB stack, threshold and measure the applicable area on only the green channel were used to quantify the area containing positive staining. This value was then normalized using the total area (height, i.e. thickness multiplied by culture width) of the organotypic cultures to account for differences in size.

4.6 | Western blot analysis

Cell lysates were collected from confluent WT, pCLDN1 KO and clone cells (A8, H1 and D5) differentiated in high Ca^{2+} media for claudin-1 protein expression. Cells were lysed using radioimmunoprecipitation assay (RIPA) buffer (Boston BioProducts, Ashland, MA, USA) containing protease/phosphatase inhibitors with 0.2% SDS. Samples were then run on a NuPAGE™ 4%–12% Bis-Tris protein gel (ThermoFisher Scientific) and transferred to a PVDF membrane. Membranes were probed with both anti-claudin-1 (#51-9000, 1:1000 dilution) and anti-β-actin HRP (#sc-47778 HRP, 1:5000 dilution) as a housekeeping protein control. Anti-claudin-1 was detected with anti-rabbit IgG HRP (Cytiva, Marlborough, MA, USA). Detected proteins were visualized using the SuperSignal West Pico PLUS Chemiluminescent Substrate (ThermoFisher Scientific) and imaged on a BioRad Gel Imaging System (Bio-Rad). Input (10 μg) was normalized by protein content using the Pierce® BCA Protein Assay Kit (ThermoFisher Scientific).

4.7 | Transepithelial electrical resistance (TEER) and electrical impedance spectroscopy (EIS)

TEER on monolayer cultures was done as previously published.[41] Measurements were taken at the same time each day after differentiation was induced. For organotypic cultures, EIS was used to measure real-time electrical impedance using the Locsense Artemis (Locsense, Enschede, The Netherlands) equipped with a SmartSense lid for monitoring cells in conventional transwell plates containing inserts (Nunc, ThermoFisher Scientific). After lowering of Day 10 air exposed organotypic cultures to the middle position of the culture plate, 500 μL of PBS was added on top of the organotypic cultures and the transwell plate was transferred to a new 24-well plate containing 1.6 mL PBS per well. Following calibration, continuous impedance (Ω, Ohms) was measured while sweeping frequency from 10 Hz to 100 000 Hz. Afterwards, measured impedance was corrected for blank impedance per electrode and corrected for culture insert size (0.47 cm^2), resulting in impedance multiplied by square centimetre values ($\Omega \cdot cm^2$). Mean impedance at four frequencies (620 Hz, 853 Hz, 1172 Hz and 1609 Hz) was used to determine differences between WT, pCLDN1 KO and A8 clone cells.

4.8 | Permeability assay

Paracellular flux across cell monolayers was assessed using FITC Dextran of different molecular weights to test for barrier disruption.[17] 75 000 N/TERT-2G cells were plated in a 24-well format transwell system (Corning Incorporated, Cat# 3470) and incubated for 48 h to reach confluency. Cells were induced to differentiate and permeability was tested 24, 48 and 72 h later. To determine changes to the leak or unrestricted pathways for paracellular permeability, FITC Dextran of 4 kDa or 40 kDA (Sigma-Aldrich) was used, respectively. FITC Dextran at 200 μg/mL was added to the upper chamber of the transwell system, which contained either WT or claudin-1-lacking cells. The plates were incubated at 37°C in the dark for 2 h. A 50 μL sample was removed from the lower chamber of the transwell after 2 h and added to a clear bottom 96-well plate to measure fluorescence (Ex: 490 nm, Em: 525 nm) using a Spectramax i3x

Multi-Mode Plate Reader (Molecular Devices, San Jose, CA, USA). Macromolecule flux was calculated using the apparent permeability coefficient (P_{app}, cm/s) as previously published.[43]

4.9 | qPCR

WT, pCLDN1 KO, A8, H1 and D5 cells were plated in 24-well plates, grown to confluency and differentiated or left undifferentiated as described above. To isolate mRNA, cells were washed with PBS, and then 250 μL of TRI Reagent Solution (ThermoFisher Scientific) was added to each well for 5 min. Wells were scraped with a P1000 micropipette tip and transferred to Eppendorf tubes. mRNA was isolated from cells using the E.Z.N.A Total RNA Kit (Omega Bio-Tek, Norcross, GA, USA), resuspended in nuclease free water and then quantified as described above. cDNA synthesis was performed with 300 ng of mRNA per reaction using the qScript cDNA synthesis kit (Quantabio, Beverly, MA, USA). The PCR amplification protocol for cDNA synthesis was as follows: 22°C for 5 min, 42°C for 30 min and 85°C for 5 min. Samples were then prepared for qPCR using 5 μL PerfeCTa SYBR Green SuperMix (Quantabio, Beverly, MA, USA), 3.6 μL nuclease free water, 1 μL primer and 0.4 μL cDNA and run on a iCycler iQ Real-Time PCR Detection System (Bio-Rad) using the following protocol: 94°C for 3 min, 39cycles 94°C for 15 s and 55°C for 1 min, 95°C for 1 min, 55°C for 55 s and 55°C for 5 s. Primer sequences for each gene transcript investigated are provided in Table S1. Data are shown as either ΔCq (gene of interest – housekeeping gene [*HPRT1*]) or relative mRNA expression calculated as $2^{-\Delta\Delta Cq}$, which is derived from CLDN1 KO cells compared to WT controls.[44]

4.10 | Data and statistical analysis

Benchling was used to prepare Figure 1A (Benchling, San Francisco, CA, USA). Clustal Omega provided sequencing alignment of WT and *CLDN1* edited genes. All statistical tests and graphs were completed with GraphPad Prism software v9.4.1. Statistical differences were detected using a two-tailed paired *t*-test between WT and pCLDN1 KO or an ANOVA analysis comparing the WT claudin-1 expressing cells (either WT -gRNA or B6 clone cells) to the CLDN1 KO cells (pCLDN1 KO, A8 and H1).

AUTHOR CONTRIBUTIONS

Conceptualization, M.G.B.; methodology, K.A.A., H.S., I.V.W., D.R.O., J.P.H.S., and M.G.B.; validation, K.A.A., J.P.H.S., and M.G.B.; formal analysis, K.A.A., J.P.H.S., and M.G.B.; investigation, K.A.A., M.C.M., H.S., I.V.W., D.R.O., J.P.H.S., and M.G.B.; writing—original draft preparation, K.A.A., M.C.M., and M.G.B.; writing—review and editing, K.A.A., M.C.M., J.P.H.S., M.G.B.; visualization, K.A.A., J.P.H.S., and M.G.B.; supervision, J.P.H.S. and M.G.B.; project administration, J.P.H.S. and M.G.B.; funding acquisition, J.P.H.S. and M.G.B. All authors have read and agreed to the published version of the manuscript.

ACKNOWLEDGEMENTS

We would like to acknowledge Dr. James G. Rheinwald for providing access to N/TERT-2G cells. We would also like to acknowledge Dr. Josh Munger for allowing us to use his Neon Electroporator for establishing our CRISPR/Cas9 gene-edited cell lines. Additionally, we would like to thank Dr. Lisa Beck and Dr. Ellen H. van den Bogaard for providing oversight on the development of this project. MCM is supported by the National Institute of Allergy and Infectious Disease (T32 AI007285, T32 AI118689). HS was provided support by the de Kiewiet Summer Research Fellowship, a University of Rochester funding mechanism for undergraduate research. JPHS is supported by LEO foundation grant LF18068 and MGB is supported by the Department of Dermatology, University of Rochester Medical Center. This work was made possible by a generous donation from an anonymous donor.

FUNDING INFORMATION

No external funding was used for the studies herein.

CONFLICT OF INTEREST STATEMENT

All authors state no conflict of interest.

DATA AVAILABILITY STATEMENT

The data that support the findings of this study are available from the corresponding author upon reasonable request.

ORCID

Kimberly A. Arnold https://orcid.org/0000-0002-7633-8732
Mary C. Moran https://orcid.org/0000-0002-6456-082X
Huishan Shi https://orcid.org/0000-0002-2231-7151
Ivonne M. J. J. van Vlijmen-Willems https://orcid.org/0000-0002-3522-2573
Diana Rodijk-Olthuis https://orcid.org/0000-0002-7752-6209
Jos P. H. Smits https://orcid.org/0000-0003-0915-8624
Matthew G. Brewer https://orcid.org/0000-0001-7631-5234

REFERENCES

1. Elias PM. Structure and function of the stratum-Corneum permeability barrier. *Drug Dev Res*. 1988;13(2–3):97-105.
2. Niessen CM. Tight junctions/adherens junctions: basic structure and function. *J Invest Dermatol*. 2007;127(11):2525-2532.
3. Ansel J, Perry P, Brown J, et al. Cytokine modulation of keratinocyte cytokines. *J Invest Dermatol*. 1990;94(6 Suppl):101S-107S.
4. Jiang Y, Tsoi LC, Billi AC, et al. Cytokinocytes: the diverse contribution of keratinocytes to immune responses in skin. *JCI Insight*. 2020;5(20):e142067.
5. Furuse M, Hata M, Furuse K, et al. Claudin-based tight junctions are crucial for the mammalian epidermal barrier: a lesson from claudin-1-deficient mice. *J Cell Biol*. 2002;156(6):1099-1111.
6. Bergmann S, von Buenau B, Vidal YSS, et al. Claudin-1 decrease impacts epidermal barrier function in atopic dermatitis lesions dose-dependently. *Sci Rep*. 2020;10(1):2024.
7. Tokumasu R, Yamaga K, Yamazaki Y, et al. Dose-dependent role of claudin-1 in vivo in orchestrating features of atopic dermatitis. *Proc Natl Acad Sci U S A*. 2016;113(28):E4061-E4068.

8. Hadj-Rabia S, Baala L, Vabres P, et al. Claudin-1 gene mutations in neonatal sclerosing cholangitis associated with ichthyosis: a tight junction disease. *Gastroenterology*. 2004;127(5):1386-1390.
9. De Benedetto A, Rafaels NM, McGirt LY, Ivanov AI, Georas SN, Cheadle C, et al. Tight junction defects in patients with atopic dermatitis. *J Allergy Clin Immunol* 2011;127(3):773–86 e1-7, 786.e7.
10. Dickson MA, Hahn WC, Ino Y, et al. Human keratinocytes that express hTERT and also bypass a p16(INK4a)-enforced mechanism that limits life span become immortal yet retain normal growth and differentiation characteristics. *Mol Cell Biol*. 2000;20(4):1436-1447.
11. Moran MC, Pandya RP, Leffler KA, Yoshida T, Beck LA, Brewer MG. Characterization of human keratinocyte cell lines for barrier studies. *JID Innov*. 2021;1(2):100018.
12. Smits JPH, Niehues H, Rikken G, et al. Immortalized N/TERT keratinocytes as an alternative cell source in 3D human epidermal models. *Sci Rep-Uk*. 2017;7:7.
13. Kim S, Kim D, Cho SW, Kim J, Kim JS. Highly efficient RNA-guided genome editing in human cells via delivery of purified Cas9 ribonucleoproteins. *Genome Res*. 2014;24(6):1012-1019.
14. Shi H, Smits JPH, van den Bogaard EH, Brewer MG. Research techniques made simple: delivery of the CRISPR/Cas9 components into epidermal cells. *J Invest Dermatol*. 2021;141(6):1375-1381. e1.
15. Seki A, Rutz S. Optimized RNP transfection for highly efficient CRISPR/Cas9-mediated gene knockout in primary T cells. *J Exp Med*. 2018;215(3):985-997.
16. Sunagawa GA, Sumiyama K, Ukai-Tadenuma M, et al. Mammalian reverse genetics without crossing reveals Nr3a as a short-sleeper gene. *Cell Rep*. 2016;14(3):662-677.
17. Kirschner N, Haftek M, Niessen CM, et al. CD44 regulates tight-junction assembly and barrier function. *J Invest Dermatol*. 2011;131(4):932-943.
18. Brunner PM, Leung DYM, Guttman-Yassky E. Immunologic, microbial, and epithelial interactions in atopic dermatitis. *Ann Allerg Asthma Im*. 2018;120(1):34-41.
19. Danso MO, van Drongelen V, Mulder A, et al. TNF-alpha and Th2 cytokines induce atopic dermatitis-like features on epidermal differentiation proteins and stratum corneum lipids in human skin equivalents. *J Invest Dermatol*. 2014;134(7):1941-1950.
20. Ghosh D, Ding L, Sivaprasad U, et al. Multiple transcriptome data analysis reveals biologically relevant atopic dermatitis signature genes and pathways. *PLoS One*. 2015;10(12):e0144316.
21. Kuo IH, Carpenter-Mendini A, Yoshida T, et al. Activation of epidermal toll-like receptor 2 enhances tight junction function: implications for atopic dermatitis and skin barrier repair. *J Invest Dermatol*. 2013;133(4):988-998.
22. Raya-Sandino A, Lozada-Soto KM, Rajagopal N, et al. Claudin-23 reshapes epithelial tight junction architecture to regulate barrier function. *Nat Commun*. 2023;14(1):6214.
23. Gerdes J, Schwab U, Lemke H, Stein H. Production of a mouse monoclonal antibody reactive with a human nuclear antigen associated with cell proliferation. *Int J Cancer*. 1983;31(1):13-20.
24. Kirschner N, Rosenthal R, Furuse M, Moll I, Fromm M, Brandner JM. Contribution of tight junction proteins to ion, macromolecule, and water barrier in keratinocytes. *J Invest Dermatol*. 2013;133(5):1161-1169.
25. Sugawara T, Iwamoto N, Akashi M, et al. Tight junction dysfunction in the stratum granulosum leads to aberrant stratum corneum barrier function in claudin-1-deficient mice. *J Dermatol Sci*. 2013;70(1):12-18.
26. Tokumasu R, Tamura A, Tsukita S. Time- and dose-dependent claudin contribution to biological functions: lessons from claudin-1 in skin. *Tissue Barriers*. 2017;5(3):e1336194.
27. Kirschner N, Houdek P, Fromm M, Moll I, Brandner JM. Tight junctions form a barrier in human epidermis. *Eur J Cell Biol*. 2010;89(11):839-842.
28. van Neste D, Douka M, Rahier J, Staquet MJ. Epidermal changes in atopic dermatitis. *Acta Derm Venereol Suppl (Stockh)*. 1985;114:67-71.
29. Gruber R, Bornchen C, Rose K, et al. Diverse regulation of claudin-1 and claudin-4 in atopic dermatitis. *Am J Pathol*. 2015;185(10):2777-2789.
30. Krueger JG, Fretzin S, Suarez-Farinas M, et al. IL-17A is essential for cell activation and inflammatory gene circuits in subjects with psoriasis. *J Allergy Clin Immunol*. 2012;130(1):145-154. e9.
31. Wolk K, Haugen HS, Xu W, et al. IL-22 and IL-20 are key mediators of the epidermal alterations in psoriasis while IL-17 and IFN-gamma are not. *J Mol Med (Berl)*. 2009;87(5):523-536.
32. Lowes MA, Suarez-Farinas M, Krueger JG. Immunology of psoriasis. *Annu Rev Immunol*. 2014;32:227-255.
33. Sakurai K, Sugiura H, Matsumoto M, Uehara M. Occurrence of patchy parakeratosis in normal-appearing skin in patients with active atopic dermatitis and in patients with healed atopic dermatitis: a cause of impaired barrier function of the atopic skin. *J Dermatol Sci*. 2002;30(1):37-42.
34. Beck LA, Thaci D, Hamilton JD, et al. Dupilumab treatment in adults with moderate-to-severe atopic dermatitis. *N Engl J Med*. 2014;371(2):130-139.
35. Chovatiya R, Paller AS. JAK inhibitors in the treatment of atopic dermatitis. *J Allergy Clin Immunol*. 2021;148(4):927-940.
36. Wollenberg A, Blauvelt A, Guttman-Yassky E, et al. Tralokinumab for moderate-to-severe atopic dermatitis: results from two 52-week, randomized, double-blind, multicentre, placebo-controlled phase III trials (ECZTRA 1 and ECZTRA 2). *Br J Dermatol*. 2021;184(3):437-449.
37. Guttman-Yassky E, Bissonnette R, Ungar B, et al. Dupilumab progressively improves systemic and cutaneous abnormalities in patients with atopic dermatitis. *J Allergy Clin Immunol*. 2019;143(1):155-172.
38. Smith SH, Jayawickreme C, Rickard DJ, et al. Tapinarof is a natural AhR agonist that resolves skin inflammation in mice and humans. *J Invest Dermatol*. 2017;137(10):2110-2119.
39. Smits JPH, Ederveen THA, Rikken G, et al. Targeting the cutaneous microbiota in atopic dermatitis by coal tar via AHR-dependent induction of antimicrobial peptides. *J Invest Dermatol*. 2020;140(2):415-424.e10.
40. van den Bogaard EH, Bergboer JG, Vonk-Bergers M, et al. Coal tar induces AHR-dependent skin barrier repair in atopic dermatitis. *J Clin Invest*. 2013;123(2):917-927.
41. Brewer MG, Yoshida T, Kuo FI, Fridy S, Beck LA, De Benedetto A. Antagonistic effects of IL-4 on IL-17A-mediated enhancement of epidermal tight junction function. *Int J Mol Sci*. 2019;20(17):4070.
42. Moran MC, Pope EM, Brewer MG, Beck LA. Supply chain disruptions during COVID-19 pandemic uncover differences in keratinocyte culture media. *JID Innov*. 2022;2(6):100151.
43. Pongkorpsakol P, Turner JR, Zuo L. Culture of intestinal epithelial cell monolayers and their use in multiplex macromolecular permeability assays for in vitro analysis of tight junction size selectivity. *Curr Protoc Immunol*. 2020;131(1):e112.
44. Livak KJ, Schmittgen TD. Analysis of relative gene expression data using real-time quantitative PCR and the 2(T)(-Delta Delta C) method. *Methods*. 2001;25(4):402-408.

SUPPORTING INFORMATION

Additional supporting information can be found online in the Supporting Information section at the end of this article.

Figure S1. Isolation and characterization of CLDN1 KO clones. (A) PCR amplification and gel electrophoresis of the *CLDN1* sequence from the CLDN1 KO clones 'A8', 'H1' and 'D5' and WT cells. (B) DNA sequencing of the clones compared to a WT clone from the CRISPR/Cas9 editing reaction. The top DNA sequence is WT *CLDN1* and the

bottom sequence is the clone *CLDN1* sequence with '*' representing matching nucleotides. The dashes indicate the deletion in *CLDN1* present in the different clones. (C) Western blot expression of claudin-1 in WT compared to different claudin-1 lacking clones 'A8', 'H1' and 'D5' from differentiated KC.

Figure S2. mRNA expression changes substantially after KC are exposed to high Ca^{2+}. ΔCq values of representative genes for (A) barrier proteins, (B) differentiation markers and (C) cytokines depicted in Figure 3 ($n = 5$ experiments). Gene of interest expression was normalized to expression of the housekeeping gene *HPRT1*. Statistical differences were evaluated by paired t-tests. Data are shown as mean ± SEM. $^{*}p < 0.05$, $^{**}p < 0.01$.

Figure S3. CLDN1 KO clones have similar mRNA expression to pCLDN1 KO cells. Gene expression in ΔCq of representative (A) barrier proteins, (B) differentiation markers and (C) cytokines in early differentiated submerged monolayer cultures of KC. Gene expression levels in pCLDN1 KO cells and three clonal lines (A8, H1 and D5) measured by qPCR and normalized to *HPRT1* levels ($n = 2$ experiments). Individual experimental means are shown.

Table S1. Primers sequences used for qPCR.

How to cite this article: Arnold KA, Moran MC, Shi H, et al. *CLDN1* knock out keratinocytes as a model to investigate multiple skin disorders. *Exp Dermatol*. 2024;33:e15084. doi:10.1111/exd.15084